Expression and Intracellular Distribution of Stress Fibers in Aortic Endothelium

Glenn E. White and Keigi Fujiwara

Department of Anatomy and Cellular Biology, Harvard Medical School, Boston, Massachusetts 02115. Dr. White's present address is Laboratory of Molecular and Cellular Cardiology, The Children's Hospital, Boston, Massachusetts 02115.

Abstract. Immunofluorescence microscopy was used to determine the number of endothelial cells with stress fibers for three age groups, and for three distinct anatomical locations within the descending thoracic aorta of both normotensive and spontaneously hypertensive rats. For each age group examined, hypertensive rats consistently demonstrated greater stress fiber expression than did normotensive rats. Neither age nor blood pressure was the predominant influence on stress fiber expression in aortic endothelium. In the normotensive rats, stress fiber expression remained unchanged for all age groups examined. For both strains, however, more endothelial cells with stress fibers were found in those regions where fluid shear stresses are expected to be high, when compared with those regions where the fluid shear stresses are expected to be low. This observation suggests that anatomical location, with its implied differences in fluid shear stress levels, is a major influence on stress fiber expression within this tissue. Electron microscopy was used to determine the intracellular distribution of stress fibers for both strains. Most stress fibers in both strains were located in the abluminal portion of the endothelial cells. This result is consistent with a role for stress fibers in cellular adhesion. However, the hypertensive rats had a higher proportion of stress fibers in the luminal portion of their cytoplasm than the normotensive rats. This increased presence of stress fibers in the luminal portion of the cell may be important in maintaining the structural integrity of the endothelial cell in the face of elevated hemodynamic forces in situ.

STRESS fibers were originally described by Lewis and Lewis (30) in vascular endothelial cells maintained in tissue culture. Subsequently, many investigators studied stress fibers in other types of cultured cells with both the light and the electron microscope (for an example, see reference 4). These phase-dense, linear structures consist of antiparallel arrays of microfilaments (3, 46). The antibody-staining technique has demonstrated that stress fibers contain actin (28) and myosin (16, 50), as well as several other accessory contractile proteins (for a review, see reference 6). Until recently, however, the existence of this structure within the cells of a tissue had not been unequivocally demonstrated. Stress fibers that occur in cells in situ were first characterized, using immunofluorescence microscopy, in the scleroblasts of the fish scale (5). Subsequently, stress fibers were demonstrated in vascular endothelium in situ (18, 22, 45, 55, 56).

Since stress fibers were primarily studied in tissue cultured cells, speculation as to their potential physiologic roles has mainly come from these in vitro studies. One of the primary stress fiber functions is a role in cell adhesion to the substrate. The relationship between stress fibers and adhesion plaques was extensively studied (1, 19, 31, 35, 51). In cultured cells, most stress fibers terminate at an adhesion plaque, which is the area of the tightest adhesion between a cell and its substrate. These observations strongly suggest that stress fibers play an important role in cell–substrate adhesion. These in vitro studies have led some investigators to postulate a role for the in situ stress fiber in cellular adhesion (5, 19, 45, 55, 56).

To further probe the function of stress fibers in cells in situ, the aortic endothelial cells of the spontaneously hypertensive (SHR)[1] rat (Okamoto–Aoki type [40]) were used as a model system. These animals have been extensively studied, and many of their physiologic and pathologic characteristics are known (40, 43, 44, 49; for reviews, see references 39 and 57). Previous studies in our laboratory (55) demonstrated a marked increase in stress fiber expression in the endothelial cells lining the thoracic aorta of the SHR when compared with the age-matched (8 wk) and sex-matched Wistar-Kyoto (WKY) rat (normotensive control). The state of hypertension can be experimentally induced in laboratory animals by a variety of methods (21, 32, 42), and the influence of experimentally induced hypertension on various aspects of endothelial structure and function has been extensively studied (2, 8, 17, 20, 23, 47, 48). Using such model systems of hypertension, some have reported an increase in the number of "cross-striated microfilament bundles" in en-

1. *Abbreviations used in this paper*: Regions 1, 2, and 3, R_1, R_2, and R_3; SHR, spontaneously hypertensive rat; WKY, Wistar-Kyoto rat.

dothelium 1 wk after these animals were rendered hypertensive (17, 20, 48).

When one considers the factors that could account for this increase in stress fiber expression in both genetically based and experimentally induced hypertension, blood pressure figures prominently. Therefore, it is important to determine whether there is a direct correlation between the magnitude of the blood pressure and stress fiber expression. It is also important to determine whether the greater stress fiber expression in the 8-wk-old hypertensive rats (55) is a temporary phenomenon or persists for an extended period of time. To answer these two questions, stress fiber expression was quantified within the WKYs and SHRs at three different age groups: 5, 10, and 20 wk. This design of the experiment allowed us to study the influence of increasing age and blood pressure on stress fiber expression. It is important to note that SHRs are not hypertensive at birth; their initial elevated blood pressure appears at 5–6 wk old, and then increases until the animal is ~15 wk old (49).

The potential influence of the other principal hemodynamic force, fluid shear stress, must also be considered. While fluid shear stress levels in these animals have not been directly measured, other physical characteristics have been measured (9, 49) from which one can estimate the level of fluid shear stress. It is generally agreed that this force should always be elevated in SHRs when compared with WKYs. The influence of fluid shear stress on stress fiber expression can also be studied within a particular animal. For example, in vitro studies of blood vessel models have demonstrated that fluid shear stresses can vary from region to region within the vessel (11, 33). In particular, branch points and regions of sharp vessel wall curvature are two regions where shear stresses are highest within the vessel (11, 33). Thus, stress fiber expression in three distinct regions of the thoracic aorta was quantified. Two of these regions were near the ostia of the intercostal arteries and were expected to have higher shear stress levels when compared with the region away from the branch point.

If stress fibers play a role in cellular adhesion in situ, then one might expect them to be located in the abluminal (basal) portion of the endothelial cell's cytoplasm. Thus, an electron microscopic study was carried out to quantitate the intracellular distribution of stress fibers within the aortic endothelium of both WKYs and SHRs.

The results presented in this paper demonstrate that the expression of stress fibers in aortic endothelial cells in situ is not directly related to increasing age or blood pressure. The data suggest that anatomical location, reflecting the levels of fluid shear stresses at these locations, may be one of the major influences on stress fiber expression. In addition, our study demonstrates that most stress fibers are located in the abluminal cytoplasm, but that they are not limited to that region. These results are consistent with a role for stress fibers in cellular adhesion in situ, but they also suggest that this structure plays a role in maintaining the structural integrity of the endothelium. The study of stress fiber expression at different ages was first presented at the 23rd Meeting of the American Society for Cell Biology (53). The electron microscopic studies were presented at the Third International Congress for Cell Biology in Tokyo, Japan (September, 1984).

Materials and Methods

Experimental Animals

Male WKYs and SHRs (4, 8, and 18 wk) were purchased from Taconic Farms Inc. (Germantown, NY). For both strains, there was a total of 11 animals in each age group. The animals were housed in the department's animal facility until they reached the ages (5, 10, and 20 wk) used for the studies. All animals were maintained on a diet of laboratory rat chow (Ralston Purina Co., St. Louis, MO) and tap water ad libitum.

Blood Pressure Measurements and Fixation Procedures

Animals were anesthetized with ether, and their blood pressures (mean arterial pressure) were measured with a mercury manometer via cannulation of the femoral artery. The animals were then perfusion-fixed at their mean arterial pressure as previously described (12, 55). For the immunofluorescence microscopy studies, the blood vessel was fixed for 15 min with 2% formaldehyde/0.1% picric acid/50 mM sodium cacodylate (pH 7.4). For the electron microscopy study, the blood vessel was fixed for 10 min with the primary fixative: 2% formaldehyde/2.5% glutaraldehyde/0.01% picric acid/0.025% $CaCl_2$/100 mM sodium cacodylate (pH 7.4) (24).

Immunofluorescent Procedures

After fixation, the thoracic aorta was dissected from the animal, and then prepared for immunofluorescence microscopy as a whole mount (55). All primary antibody stainings were with antiplatelet myosin (16). The secondary antibody was rhodamine-labeled goat anti-rabbit IgG (Lot #17179; Yeda Research and Development Co. Ltd., Rehovot, Israel). Microscopy was performed on a Leitz Orthoplan epifluorescence microscope. The lens, filter combinations, and photography specifications were described elsewhere (55).

Quantitative Methods for Determining Stress Fiber Expression

For each age group, four animals of each strain were examined. The thoracic aorta, at the levels of the first through the sixth intercostal arteries, was ex-

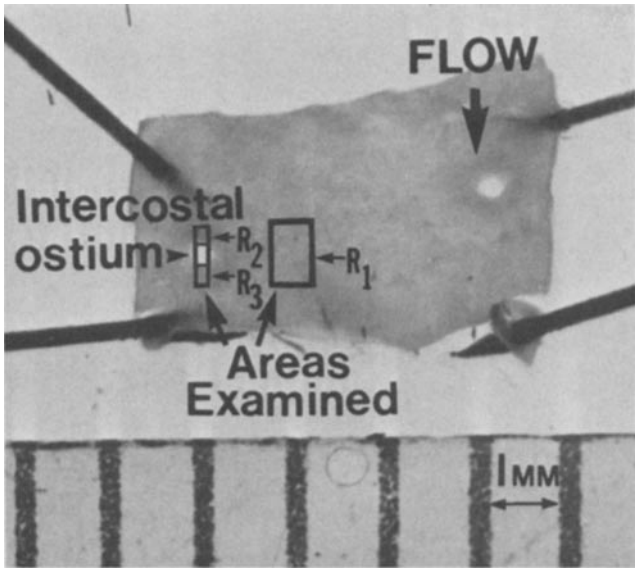

Figure 1. Specific regions of the descending thoracic aorta examined in both WKYs and SHRs. The number of endothelial cells with stress fibers in the regions designated R_1, R_2, and R_3 were quantitated and then compared. For the immunofluorescence microscopy studies, a 150 × 750-μm area in R_1 exactly 1 mm from the center of the ostia of the intercostal artery was examined. This corresponds to the right side of the rectangle that designates R_1. For the study of the intracellular distribution of stress fibers in endothelial cells, all of R_1 was used.

amined. Three regions were selected from each of these six segments (Fig. 1). For each segment, only these three areas were examined. R_1 is a 150 × 750-μm area, while R_2 and R_3 are 150 × 250-μm areas (see figure legend for exact location of R_1 in this study). All segments were examined without prior knowledge of the strain. All cells within the respective fields were scored as either positive (i.e., containing at least one stress fiber) or as negative (i.e., no detectable stress fibers). The counts were made directly on the fluorescence microscope, and 800–1,000 cells/animal were examined.

The antimyosin antibody was used for this study since the antimyosin staining pattern of stress fibers in both cultured cells and in cells in situ is characteristically striated (5, 16, 50, 55). The appearance of several striations along a linear structure was, therefore, taken as positive identification of a stress fiber. The proportion of endothelial cells with stress fibers was calculated as being the number of endothelial cells with at least one stress fiber divided by the total number of endothelial cells in the designated area. The two-sample *t* test was used to calculate the confidence level when various data groups were compared. $P < 0.05$ was used as the criterion for determining whether differences between compared data groups were real.

Electron Microscopic Procedures

After perfusion fixation with the primary fixative for 10 min, the thoracic aorta was dissected out and immersed in the same primary fixative for another 20 min. During this time, the area of interest within the aorta (R_1 in Fig. 1, see figure legend) was cut out, and its orientation to the direction of blood flow was noted. The tissue was then postfixed with 1% osmium tetraoxide. Postfixation with OsO_4 was the crucial step in preserving stress fibers. To reduce the degradative effects of OsO_4 on actin filaments (36), the tissue was postfixed with 1% OsO_4/100 mM Na-phosphate (pH 6.2) on ice for 12–15 min. Deviations from this scheme (concentration, time, temperature, or pH) led to significant deterioration of the stress fiber morphology (they were more difficult to find in the cells, and frequently failed to show their characteristic periodic density). The tissue was dehydrated with increasing concentrations of ethanol, and then embedded in Polybed 812/Araldite 6005 (Polysciences, Warrington, PA). Thin sections were cut using a diamond knife (E. I. DuPont de Nemours & Co., Sorvall Instruments Div., Newtown, CT) and an MT2-B Porter Blum Ultramicrotome (Sorvall Instruments Div.). The sections were mounted on 300-mesh copper grids (Polysciences Inc.), stained with 2% aqueous uranyl acetate for 15 min (17), and then stained again with 1% lead citrate for 1 min. All microscopy was performed on either a JEOL 100B or 100S electron microscope.

Quantitative Methods for Determining Stress Fiber Distribution

For each age group, five animals of each strain were examined. The region corresponding to R_1 (Fig. 1) from the first and the sixth aortic rings was used to determine the distribution of stress fibers within the cytoplasm of the endothelial cells. The sampling was performed as follows. First, the tissue was oriented for thin sectioning such that the plane of sectioning was perpendicular to the major axis of the endothelial cell. When cells were cut in this orientation, stress fibers were cut in cross-section. Second, the blocks were sectioned, and the sections stained, and then examined on the electron microscope. Only one section per grid was used for the study, and only those cells with their nuclei included were photographed. After the examination of the first set of grids was completed, the blocks were retrimmed and then resectioned. This second set of sections were then examined in the same manner as the first. This procedure ensured that no cell was scored twice. Approximately 45–70 cells with stress fibers were obtained for each age group. Third, the negatives were printed (54,000× final magnification), and the prints used to gather the data. All prints were examined "blind" (without knowledge of the strain). Using the nucleus as the reference point, we drew a line bisecting the cell and classified stress fibers as either (*a*) abluminal (being below this line), (*b*) luminal (being above this line), or (*c*) midline (spanning this line).

When cut in cross-section, a stress fiber appeared as a "cluster of dots" (if sectioned in near perfect cross-sectional orientation) or sometimes as a smeared cytoplasmic density (when the sectioning plane was off from the perfect cross-section). In addition to this characteristic appearance, the diameter (>0.15 μm) of such clusters was another useful criterion for identification of a stress fiber. In the regions where the stress fibers were located, cytoplasmic organelles were excluded, and the staining was darker than the adjacent areas. The lack of a membrane surrounding a cytoplasmic density was useful in separating stress fibers from Weibel-Palade bodies found in vascular endothelium (52). After all cells were examined, the data were decoded and tabulated for each strain. The proportion of luminal, abluminal, and midline stress fibers was determined by dividing the total number of stress fibers in each category by the total number of stress fibers observed.

Results

Physical Characteristics of WKYs and SHRs

To ascertain that the normotensive and the spontaneously hypertensive rats obtained from the supplier had a typical phenotypic expression of the respective strains, body weight and mean arterial blood pressure of each animal were recorded immediately before their perfusion fixation. These values were compiled and analyzed as shown in Table I. Growth charts and blood pressure readings provided by the supplier indicated that these animals were within the normal weight and blood pressure ranges for their respective age groups. The results of the two-sample *t* test indicated that the differences in weights between age-matched WKYs and SHRs were not significant. These data support the observation that the hypertension in the SHR is not based on obesity (40).

For comparison of the blood pressure between the age-matched WKYs and SHRs, the two-sample *t* test was also used. The calculated confidence levels at 5, 10, and 20 wk were $P < 0.05$, $P < 0.01$, and $P < 0.01$, respectively. The inference from the statistical treatment of the blood pressure differences is that they are real at all ages. These mean arterial blood pressure values are in agreement with a previous study where the same ages and anesthetic have been used (26). Comparisons can also be made among the blood pressures of the three age groups within the same strain. The calculation of the confidence level from the two-sample *t* test indicated that the differences among the WKY age groups were not real. For SHRs, while the differences between the 5- and 10-wk-old animals were not real, the differences between 5 and 20 wk, and 10 and 20 wk were real ($P < 0.01$).

Friedman (14) approximated mean arterial blood pressure as 1/3 systolic pressure plus 2/3 diastolic pressure. Using this relationship, one can estimate the 5-wk SHRs' systolic pressure as >150 mmHg, the recognized standard for hypertension (57). These observations indicated that the SHRs purchased were indeed hypertensive, and that the WKY and SHR strains used in this study were physiologically different.

Proportion of Endothelial Cells with Stress Fibers

For both the normotensive and the spontaneously hyperten-

*Table I. Physical Characteristics of WKYs and SHRs**

Strain	Age	Weight	Blood pressure
	wk	*g*	*mmHg*‡
WKY	5	98 ± 2	108 ± 5
SHR	5	102 ± 3	120 ± 3
WKY	10	242 ± 4	97 ± 3
SHR	10	225 ± 2	127 ± 4
WKY	20	334 ± 5	98 ± 2
SHR	20	330 ± 7	157 ± 5

All data presented as the mean ± SE.
*WKYs and SHRs, n = 11 animals/group.
‡Mean arterial blood pressure of anesthetized animals.

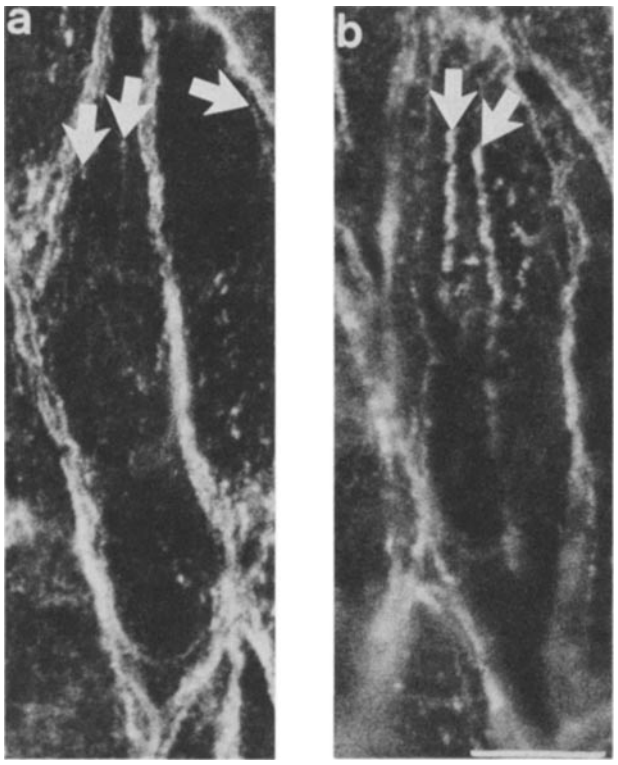

Figure 2. Antimyosin staining of aortic endothelial cells in situ. The general staining pattern includes staining of the cell cortex, which delineates cell shape. Blood flow is from top to bottom. Both cells were photographed and their images printed at the same magnification. (*a*) Stress fibers in the endothelial cell of a 5-wk WKY. While most endothelial cells in WKYs do not have stress fibers, the cells that do have them exhibit the wispy type (*arrows*). The periodic staining, characteristic of antimyosin staining of stress fibers, is apparent even in these thin fibers. (*b*) Stress fibers in 5-wk SHRs. Note the prominent stress fibers with their striations very clearly visible in the endothelial cell (*arrows*). This type of stress fiber predominates in the SHR. Bar, 10 μm.

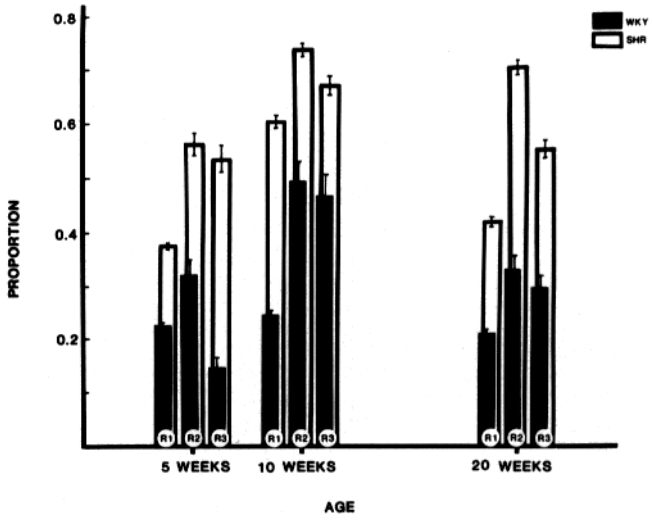

Figure 3. A histogram of the proportion of endothelial cells with stress fibers for the normotensive and hypertensive rats for the three age groups and the three regions. For all age groups, hypertensive rats have more endothelial cells with stress fibers. In addition, for all age groups, the expression of stress fibers was greater in R_2 and R_3 than in R_1. The data is presented as the mean ± SE. (See Fig. 1 for the exact location of R_1, R_2, and R_3.)

sive rats, the proportion of endothelial cells with stress fibers was determined for three regions in the vessel (Fig. 1). Region 1 (R_1) was selected as an area in which blood flow would be expected to be laminar and uniform (33). The branch points, regions 2 (R_2) and 3 (R_3) were selected because the blood flow was expected to be turbulent and the fluid shear stresses higher than in R_1 (11, 33). Comparison of stress fiber expression between regions where the fluid shear stresses are expected to be different (e.g., R_1 vs. R_2 and R_3) may shed further light on the possible influence of this hemodynamic force on the expression of stress fibers.

Most stress fibers found in WKYs, at all ages, had a thread-like appearance with an average diameter of ~0.3 μm (Fig. 2 *a*). SHRs, on the other hand, demonstrated more prominent stress fibers, with an average diameter of ~0.6 μm (Fig. 2 *b*). The periodicity of the antimyosin banding pattern was similar between these two types of stress fibers. Near branch points, the prominent stress fibers were more readily apparent in WKYs also. In addition, most stress fibers were located in the proximal (with respect to blood flow) portion of the endothelial cell.

Fig. 3 summarizes the data from the quantitative study. At every age examined, the proportion of cells with stress fibers in regions R_1, R_2, and R_3 was higher in the hypertensive rats when compared with their age-matched, normotensive controls. The inference from statistical treatment of the data (two-sample *t* test) is that all of these differences are real ($P < 0.01$).

The greatest expression of stress fibers in the hypertensive rats occurred at 10 wk. This result strongly suggests that the expression of stress fibers in vascular endothelial cells is not directly correlated with the magnitude of the blood pressure or increasing age. Since it is known that endothelial cell turnover in both normotensive and hypertensive animals is low (47), the cell turnover cannot account for these age-depen-

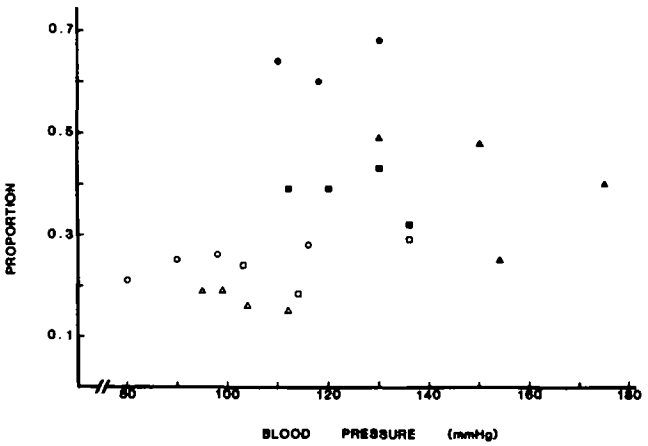

Figure 4. Plot of mean arterial blood pressure vs. the proportion of endothelial cells with stress fibers for both the WKYs and SHRs. The data indicate that a direct linear correlation between the magnitude of the blood pressure and stress fiber expression in these animals cannot be made. Open squares, WKY at 5 wk; open circles, WKY at 10 wk; open triangles, WKY at 20 wk; filled squares, SHR at 5 wk; filled circles, SHR at 10 wk; and filled triangles, SHR at 20 wk.

dent differences in expression. Thus, it appears that the stress fiber expression is dynamic so that stress fibers formed at an earlier time can be disassembled at a later time. Fig. 4 illustrates the relationship between stress fiber expression and blood pressure. The proportion of endothelial cells with stress fibers in R_1 for both WKYs and SHRs is plotted against the mean arterial blood pressure of each rat. For WKYs, the plot shows that stress fiber expression is essentially independent of the magnitude of the blood pressure. For SHRs, stress fiber expression does not remain constant; however, it cannot be directly correlated with the magnitude of the blood pressure. Linear regression analysis of the data presented in Fig. 4 gives a correlation coefficient of 0.38, indicating that a straight line cannot be drawn through the data points on this plot. Thus, based on the data, one can argue that blood pressure cannot be the primary influence on stress fiber expression in aortic endothelium.

When the proportions of endothelial cells with stress fibers for R_1, R_2, and R_3 were compared (Fig. 3), R_2 and R_3 had always higher proportions than R_1 in both strains. The only exception was the 5-wk-old WKYs where R_3 showed much lower proportion than either R_1 or R_2. The significance of this particular difference is unclear. The inference from statistical analyses of these differences in R_1, R_2, and R_3 is that they were real (two-sample t test, $P < 0.01$). Since the fluid shear stress is expected to be higher in R_2 and R_3 than in R_1, these results suggest that stress fiber expression is greater in those regions where the shearing stresses are heightened.

Quantification of Intracellular Stress Fiber Distribution

Endothelial cells exposed to high levels of fluid shear stress may need to develop a mechanism that increases their adhesion to the basement membrane. Since stress fibers in tissue culture cells appear to play a role in cell–substrate adhesion, it is possible that the stress fiber in the aortic endothelium is also involved in cellular adhesion. For the in situ endothelial cell stress fibers to be important for adhesion, they should be located in the abluminal cortex of the cell. Thus, the intracellular distribution of stress fibers was investigated by electron microscopy.

When endothelial cells were sectioned parallel to their long axis, stress fibers were cut longitudinally (Fig. 5). In this view, stress fibers typically had alternating dark and light regions with an approximate repeat of 0.3–0.4 μm. This periodicity corresponds well with the antimyosin banding pattern seen at the light microscopic level. Weibel-Palade bodies, an endothelial cell specific marker (52), and pinocytic vesicles were frequently observed.

To quantify the distribution of stress fibers in the endothelial cells, the aortic wall was sectioned perpendicular to the direction of blood flow, thus increasing the chances of finding stress fibers. This sectioning plane was also chosen so that the possibility of misidentifying a circumferential microfilament bundle, found along the lateral border, as a stress fiber (for a review, see reference 6) could be avoided. In such sections, the microfilaments of the stress fiber were cut in cross-section and appeared as a cluster of dots (if microfilaments were cut in perfect cross-section) or an electron-dense smear (if they were cut obliquely). In many sections, smooth muscle cells were also present. In certain cases, their microfilaments were cut in oblique-section. Comparing their appearance with the cytoplasmic densities seen in the endothelial cell served as a useful criterion for identifying stress fibers cut obliquely.

Examination of cross-sections of endothelial cells from both WKYs and SHRs at all three ages revealed that stress fibers in endothelium in situ do, in fact, run both above and below the nucleus. A luminally located stress fiber (arrowhead) is illustrated in Fig. 6 *a*. Near the stress fiber, there are several Weibel-Palade bodies that are seen as membrane-bound cytoplasmic densities. Fig. 6 *b* and *c* shows abluminal stress fibers (arrows). They are intimately associated with the basal plasma membrane. The portion of the plasma membrane associated with a stress fiber often extends further into the underlying basement membrane space. Fig. 6 *c* illustrates this particularly well. Furthermore, the region of the plasma membrane associated with stress fibers shows little morphological evidence for pinocytotic activities. These structural features suggest that the abluminal stress fibers define a special domain along the basal plasma membrane. In this regard, it is intriguing to note that the luminal stress fiber (Fig. 6 *a*) does not show an intimate association with the plasma membrane.

Most stress fibers were found abluminally in endothelial cells. This observation supports the hypothesis that stress fibers play a role in cell adhesion. Nevertheless, luminal stress fibers were also present. In fact, by immunofluorescence microscopy, it was possible to find stress fibers that ran above the nucleus. These luminal stress fibers, due to their intracellular location, are probably not involved in cell adhesion, but rather may be used to strengthen the cellular architecture.

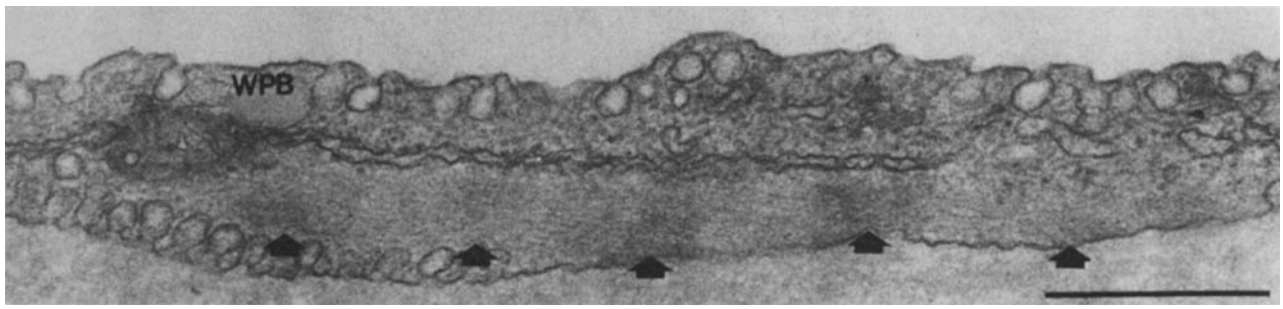

Figure 5. Longitudinal section of an endothelial cell from a hypertensive rat showing an abluminal stress fiber cut longitudinally. Periodic densities on the stress fiber, with ~0.3–0.4 μm repeats, are clearly discernible (*arrows*). WPB, Weibel-Palade body. Bar, 0.5 μm.

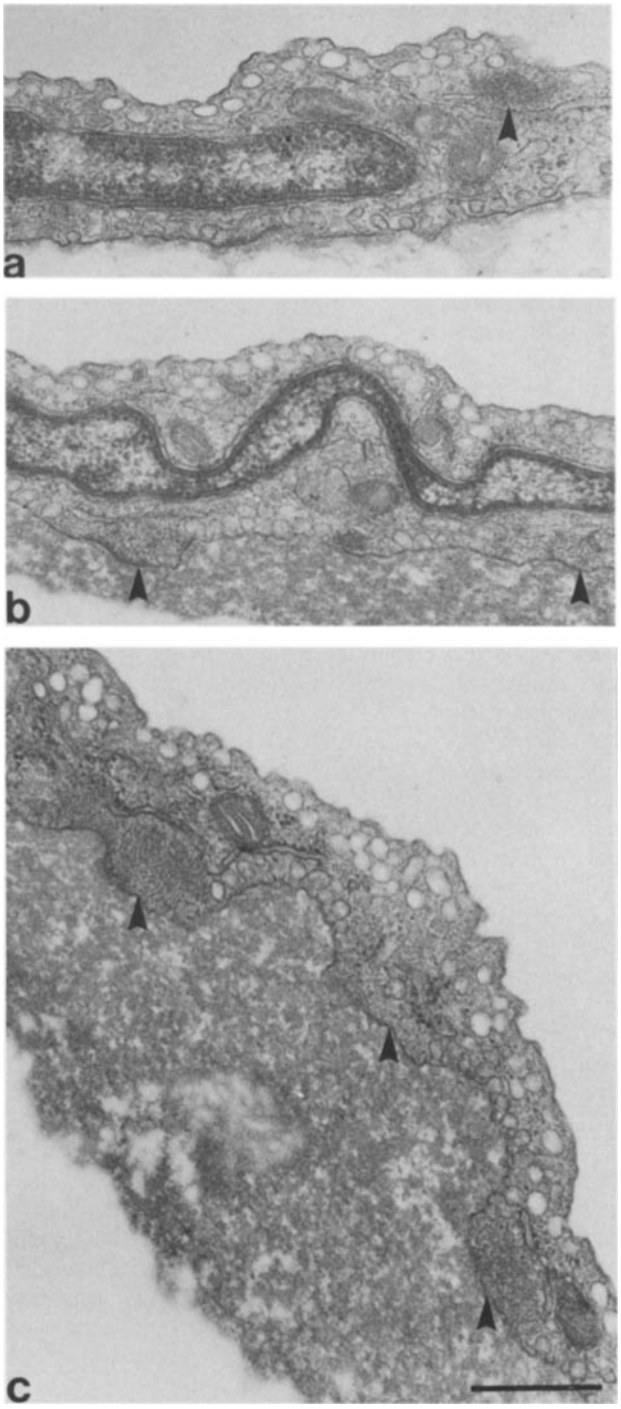

Figure 6. Examples of luminal and abluminal stress fibers in the aortic endothelial cells. Cells have been cut in cross-section. Micrographs are printed at a lower magnification than that used to gather the quantitative data. Bar, 0.5 μm. (*a*) Example of a luminal stress fiber (*arrowhead*) from a hypertensive rat. Recall that when cut in cross-section, a stress fiber will appear as a cluster of dots, or as a smeared cytoplasmic density. Note the stress fiber's proximity to the nucleus. Luminal stress fibers were typically over or near the nucleus. (*b*) Example of abluminal stress fibers. Arrowheads indicate stress fibers located in the abluminal portion of this cell and running directly underneath the nucleus. (*c*) Example of abluminal stress fibers. Arrowheads indicate abluminal stress fibers located away from the endothelial cell nucleus and near the cell periphery. This was not uncommon within the endothelium.

The cytoplasmic distribution of the stress fibers within the endothelial cells of R_1 was quantitated for both strains and all age groups. As noted in Materials and Methods, special care was taken to ensure that no cell was scored more than once. Fig. 7 summarizes the results. The differences between the age groups for each strain were not statistically significant; therefore, the data are presented as a comparison between the two strains. The inference from statistical analysis of the data was that the differences between the two strains were real (two-sample t test; $P < 0.05$). While both strains had most of their stress fibers in the abluminal portion of the endothelial cell, WKYs had a higher proportion of abluminal stress fibers than SHRs. Conversely, SHRs had a higher proportion (~50% increase) of luminal stress fibers than WKYs. Only a small proportion of stress fibers was classified as the midline type. This indicates that there is a very small number of stress fibers that span the luminal and the abluminal surfaces. The electron microscopic study also revealed that the average number of stress fibers per individual endothelial cell was approximately four for both strains and age groups. This number agrees well with that obtained from our previous immunofluorescence microscopy study (55). It is interesting to note that while both the appearance of stress fibers and the number of cells with stress fibers are different for SHRs and WKYs, the number of stress fibers per cell is the same.

Discussion

Hemodynamic Factors and Stress Fiber Expression

The data presented in this paper demonstrate that the SHR has more aortic endothelial cells with stress fibers than its age-matched normotensive counterpart. The fact that in every age group examined, SHRs had a greater number of endothelial cells with stress fibers seems to implicate blood pressure as an important influence upon the expression of stress fibers. However, Fig. 3 and 4 indicate that neither blood pressure nor age can be used to predict the proportion

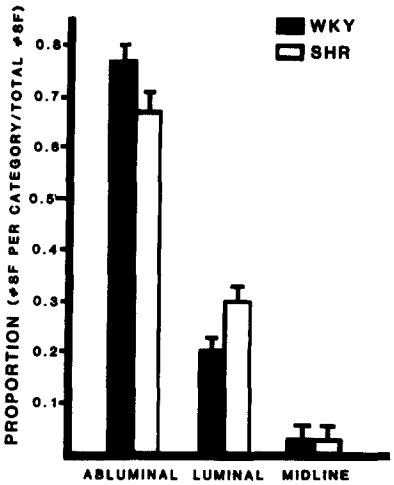

Figure 7. A histogram of proportion of luminal, abluminal, and midline stress fibers for WKYs and SHRs. The data indicate that the WKY has a higher proportion of abluminal stress fibers than the SHR. The SHR, on the other hand, has a higher proportion of luminal stress fibers. Data plotted as the mean ± SE.

of endothelial cells with stress fibers in either WKYs or SHRs. The regional variations observed in stress fiber expression within the same vessel also argue against this hypothesis. For example, R_1, R_2, and R_3 should be experiencing the same intraluminal pressure for their respective vessel segment, yet their proportions were not equal. Thus, the data indicate that blood pressure is not the primary influence upon stress fiber expression in vascular endothelial cells.

It has been suggested, however, that elevated blood pressures affect other structures within the endothelium. For example, the tight junctions of the SHR's endothelium have an approximately twofold increase in the number of junctional strands when compared with the WKY's (34). Since, as a physical force, pressure acts perpendicularly to the intima, its stretching effects on the vessel are handled primarily by the media (38). The elevated blood pressure in the SHR undoubtedly leads to greater stretching of the vessel wall during systole; therefore, this "hypertrophy" of tight junctions may serve to maintain lateral association of the endothelium in the hypertensive animal.

Fluid shear stress is the other hemodynamic force acting along the endothelial cell surface. In contrast to blood pressure, fluid shear stress results from the movement of the blood over the endothelial surface and, as such, is a frictional force that acts almost entirely upon the endothelium (38). Fluid shear stress levels must be calculated or estimated from the measurements of physical parameters such as fluid velocity, viscosity, and vessel diameter. In any blood vessel, the magnitude of the fluid shear stress is directly proportional to both blood viscosity and velocity, and inversely proportional to the vessel diameter (11). Both blood viscosity and peak flow velocities are increased in the SHR (9, 49). Studies on vessel diameter in the WKY and the SHR have shown that the diameter in the SHRs is less than or equal to the WKYs' (29, 37). Thus, the changes in these parameters observed in the SHR contribute to the increase in the level of fluid shear stress in these animals.

While there are other significant differences between the SHR and the WKY that result from the hypertensive state (for a review, see reference 39), these differences are generally systemic and could not, therefore, account for the regional variation in stress fiber expression. When comparing the three age groups within a strain, the expected shear stress values are more difficult to predict since both velocity and vessel diameter are increasing with age. Therefore, without additional studies, it is not possible to accurately predict the changes within each strain with increasing age.

Using in vitro models of blood vessels, several investigators have demonstrated that shear stress levels can vary within a vessel (for examples, see references 11, 27, 33). Of particular interest to this study is that fluid shear stresses can be significantly higher in those regions of sharp wall curvature and branch points (11, 33). That R_2 and R_3 for both strains had significantly greater stress fiber expression than R_1 is consistent with the hypothesis that fluid shear stress can affect the vascular endothelial cell's cytoskeleton. In addition, in vitro models have demonstrated that fluid shear stress can affect endothelial cell metabolism (7, 10), cell shape (54), and stress fiber expression (13, 54).

Function of Stress Fibers in Aortic Endothelium

Stress fibers have been postulated to have a role in cellular adhesion (1, 19, 31, 35, 51; for a review, see reference 6). The fact that more endothelial cells had stress fibers in an animal where the fluid shear stresses are increased, that there were more endothelial cells with stress fibers in regions of the vasculature where the shear stresses are increased, and that the majority of the stress fibers were located in the abluminal portion of the cytoplasm where they are closely associated with the specialized region of the plasma membrane support the argument that stress fibers are also involved with cellular adhesion in situ.

Earlier studies demonstrated that elevated shearing forces damage the luminal surface of the endothelium (25), and that extremely high shearing forces (350–400 dyn/cm^2) eventually de-endothelialize the aorta (15). Endothelial cells may, therefore, express stress fibers only when there is an increased demand for adhesive capability. The localization of the stress fibers in the proximal portion of the endothelial cell may also be related to an increased demand for adhesion in this part of the cell. The results in this paper suggest that the stress fibers might act in concert with the cell's ordinary adhesion machinery to increase adhesive capability.

The electron microscopic studies suggest that, in addition to adhesion, stress fibers may have another physiologic role in endothelial cells. Stress fibers have been observed in the apical portion of the cell's cytoplasm in tissue culture cells (4, 41), and our studies clearly demonstrate that such a distribution is also possible in endothelium in situ. It is difficult to assign a role for cell adhesion to these luminal stress fibers. Thus, it is postulated that the luminal stress fibers strengthen the cell in the face of elevated shear stress. Joris et al. (25) have shown that elevating the blood velocity, and, hence, the fluid shear stresses, in an animal can result in damage to the endothelium. This damage consisted of disruption of the cellular junctions, and also the disintegration of the luminal surface of the endothelium and was most common over the nucleus. As was noted, the luminal stress fibers tend to be located over or very close to the nucleus. A stress fiber in this portion of the cytoplasm could help reinforce the endothelial cell surface.

Our studies document the varying expression of stress fibers in vascular endothelium in situ. The observed differences between the normotensive and spontaneously hypertensive rats, and the regional variations observed within the endothelium, suggest that these structures were responsive to local environmental factors, principally hemodynamic forces. It is postulated that expression of these structures may be related to the endothelial cell's need for greater adhesive capability and maintenance of structural integrity.

We thank Drs. M. A. Pfeffer and M. A. Gimbrone, Jr. (Brigham and Women's Hospital, Boston, MA) for their suggestions, Dr. S. R. Bussolari (Massachusetts Institute of Technology, Cambridge, MA) for advice and valuable discussions, and Dr. W. H. Abelmann (Beth Israel Hospital, Boston, MA) for supporting G. E. White. G. E. White wishes especially to thank Mrs. Sueko White for her inspiration and moral support while this work was being completed.

This research was supported by National Institutes of Health training grant GM 07226 and HL 07374 (to G. E. White), and BRSG S07 RR 05381-20, National Science Foundation grant PCM-8119171, and National Institutes of Health grant HL 32544 (to K. Fujiwara).

Received for publication 20 March 1985, and in revised form 24 February 1986.

References

1. Abercrombie, M., and G. A. Dunn. 1975. Adhesions of fibroblasts to substratum during contact inhibition observed by interference-reflection microscopy. *Exp. Cell Res.* 92:57–62.

2. Becker, C. G., and A. M. Hardy. 1969. Contractile protein in endothelial cells of cerebral arteries and arterioles: comparison of normotensive and malignant hypertensive states. *Circulation Res.* 48 (*Suppl.* IV):44. (Abstr.)

3. Begg, D. A., R. Rodewald, and L. I. Rebhun. 1978. The visualization of actin filament polarity in thin sections. Evidence for the uniform polarity of membrane-associated filaments. *J. Cell Biol.* 79:846–852.

4. Buckley, I. K., and K. R. Porter. 1967. Cytoplasmic fibrils in living cultured cells. A light and electron microscope study. *Protoplasma.* 64:349–380.

5. Byers, H. R., and K. Fujiwara. 1982. Stress fibers in cells *in situ*: immunofluorescent visualization with antiactin, antimyosin, and anti-alpha-actinin. *J. Cell Biol.* 93:804–811.

6. Byers, H. R., G. E. White, and K. Fujiwara. 1983. Organization and function of stress fibers *in vitro* and *in situ*: a review. *Cell Muscle Motil.* 5:83–137.

7. Davies, P. F., C. F. Dewey, Jr., S. R. Bussolari, E. J. Gordon, and M. A. Gimbrone, Jr. 1984. Influence of hemodynamic forces on vascular endothelial cell function. *In vitro* studies of shear stress and pinocytosis in bovine aortic cells. *J. Clin. Invest.* 73:1121–1129.

8. De Chastonay, C., G. Gabbiani, G. Elemér, and I. Hüttner. 1983. Remodeling of the rat aortic endothelial layer during experimental hypertension. Changes in replication rate, cell density, and surface morphology. *Lab. Invest.* 48:45–52.

9. De Clerck, F., M. Beerens, L. Van Goys, and R. Xhonneux. 1980. Blood hyperviscosity in spontaneously hypertensive rats. *Thromb. Res.* 18:291–295.

10. De Forrest, J. M., and T. M. Hollis. 1978. Shear stress and aortic histamine synthesis. *Am. J. Physiol.* 234:H701–H708.

11. Dewey, C. F., Jr. 1979. Fluid mechanics of arterial flow. *Adv. Exp. Med. Biol.* 115:55–103.

12. Forssmann, W. G., S. Ito, E. Weihe, A. Aoki, M. Dym, and D. W. Fawcett. 1977. An improved perfusion fixation method for the testis. *Anat. Rec.* 188:307–314.

13. Franke, R.-P., M. Grafe, H. Schnittler, D. Seiffge, C. Mittermayer, and D. Drenckhahn. 1984. Induction of human vascular endothelial stress fibers by fluid shear stress. *Nature (Lond.).* 307:648–649.

14. Friedman, J. J. 1976. The systemic circulation. In *Physiology*. E. E. Selkurt, editor. Little, Brown & Co., Boston. 361–377.

15. Fry, D. L. 1969. Acute vascular endothelial changes associated with increased blood velocity gradients. *Circ. Res.* 22:165–197.

16. Fujiwara, K., and T. D. Pollard. 1976. Fluorescent antibody localization of myosin in the cytoplasm, cleavage furrow, and mitotic spindle of human cells. *J. Cell Biol.* 71:848–875.

17. Gabbiani, G., M. C. Badonnel, and G. Rona. 1975. Cytoplasmic contractile apparatus in aortic endothelial cells of hypertensive rats. *Lab. Invest.* 32:227–234.

18. Gabbiani, G., F. Gabbiani, D. Lombardi, and S. M. Schwartz. 1983. Organization of actin cytoskeleton in normal and regenerating arterial endothelial cells. *Proc. Natl. Acad. Sci. USA.* 80:2361–2364.

19. Geiger, B., Z. Avnur, G. Rinnerthaler, H. Hinssen, and V. J. Small. 1984. Microfilament-organizing centers in areas of cell contact: cytoskeletal interactions during cell attachment and locomotion. *J. Cell Biol.* 99(Suppl.): 83s–91s.

20. Giacomelli, F., J. Wiener, and D. Spiro. 1970. Cross-striated arrays of filaments in endothelium. *J. Cell Biol.* 45:188–192.

21. Goldblatt, H., J. Lynch, R. F. Hanzel, and W. W. Summerville. 1934. Studies on experimental hypertension. I. Production of persistent elevation of systolic blood pressure by means of renal ischemia. *J. Exp. Med.* 59:347–379.

22. Herman, I. M., T. D. Pollard, and A. J. Wong. 1982. Contractile proteins in endothelial cells. *Ann. NY Acad. Sci.* 401:50–60.

23. Hüttner, I., P. M. Costabella, C. De Chastonay, and G. Gabbiani. 1982. Volume, surface, and junctions of rat aortic endothelium during experimental hypertension. A morphometric and freeze fracture study. *Lab. Invest.* 46: 489–504.

24. Ito, S., and M. J. Karnovsky. 1968. Formaldehyde-glutaraldehyde fixatives containing trinitro compounds. *J. Cell Biol.* 39(2, Pt. 2):168*a* (Abstr.)

25. Joris, I., T. Zand, and G. Majno. 1982. Hydrodynamic injury of the endothelium. *Am. J. Pathol.* 106:394–408.

26. Judy, W. V., and S. K. Farrel. 1979. Arterial baroreceptor reflex control of sympathetic nerve activity in the spontaneously hypertensive rat. *Hypertension (Dallas).* 1:605–614.

27. Karino, T., and M. Motomiya. 1983. Flow visualization in isolated transparent natural blood vessels. *Biorheology.* 20:119–127.

28. Lazarides, E., and K. Weber. 1974. Actin antibody: the specific visualization of actin filaments in non-muscle cells. *Proc. Natl. Acad. Sci. USA.* 71:2268–2272.

29. Lee, R. M. K. W., J. B. Forrest, R. E. Garfield, and E. E. Daniel. 1983. Comparison of blood vessel wall dimensions in normotensive and hypertensive rats by histometric and morphometric methods. *Blood Vessels.* 20:235–244.

30. Lewis, W. H., and M. R. Lewis. 1924. Behavior of cells in tissue cultures. *In* General Cytology. E. V. Cowdry, editor, University of Chicago Press, Chicago. 385–447.

31. Lloyd, C. W., C. G. Smith, A. Woods, and D. A. Rees. 1977. Mechanisms of cellular adhesion. II. The interplay between adhesion, the cytoskeleton, and morphology in substrate attached cells. *Exp. Cell Res.* 110:427–437.

32. Loomis, D. 1946. Hypertension and necrotizing arteritis in the rat following renal infarction. *Arch. Pathol.* 41:231–268.

33. Lutz, R. J., J. N. Cannon, K. B. Bischoff, R. L. Dedrick, R. K. Stiles, and D. L. Fry. 1977. Wall shear stress distribution in a model canine artery during steady flow. *Circ. Res.* 41:391–399.

34. Majack, R. A., and R. C. Bhalla. 1981. Ultrastructural characteristics of endothelial pathways in chronic hypertension. *Hypertension (Dallas).* 3: 586–595.

35. Mangeat, P., and K. Burridge. 1984. Actin-membrane interaction in fibroblasts: what proteins are involved in this association. *J. Cell Biol.* 99 (Suppl.):95s–103s.

36. Maupin-Szamier, P., and T. D. Pollard. 1978. Actin filament destruction by osmium tetraoxide. *J. Cell Biol.* 77:837–852.

37. Mulvany, M. J., P. K. Hansen, and C. Aalkjaer. 1978. Direct evidence that greater contractility of resistance vessels in spontaneously hypertensive rats is associated with a narrower lumen, a thicker media, and a larger number of smooth muscle cell layers. *Circ. Res.* 43:854–864.

38. Nerem, R. M. 1980. Arterial fluid dynamics and interactions with the vessel walls. *In* Structure and Function of the Circulation. Vol. 2. C. J. Schwartz, N. T. Werthessen, and S. Wolf, editors. Plenum Publishing Corp., New York. 719–835.

39. Okamoto, K. 1969. Spontaneous hypertension in rats. *Int. Rev. Exp. Pathol.* 7:227–276.

40. Okamoto, K., and K. Aoki. 1963. Development of a strain of spontaneously hypertensive rats. *Jpn. Circ. J.* 27:282–293.

41. Osborn, M., T. Born, H. J. Koitsch, and K. Weber. 1978. Stereo immunofluorescence microscopy. I. Three dimensional arrangements of microfilaments, microtubules, and tonofilaments. *Cell.* 14:477–488.

42. Page, I. H. 1939. The products of persistent arterial hypertension by allophane perinephritis. *J. Am. Med. Assoc.* 113:2046–2048.

43. Pfeffer, M. A., and E. D. Frohlich. 1973. Hemodynamic and myocardial function in young and old normotensive and spontaneously hypertensive rats. *Circ. Res.* 32 (Suppl.):28–38.

44. Pfeffer, M. A., E. D. Frohlich, J. M. Pfeffer, and A. K. Weiss. 1974. Pathophysiological implications of the increased cardiac output of young spontaneously hypertensive rats. *Circ. Res.* 34 (Suppl. 1):235–244.

45. Rogers, K. M., and V. I. Kalnins. 1983. Comparison of the cytoskeleton in aortic endothelial cells *in situ* and *in vitro*. *Lab. Invest.* 49:650–654.

46. Sanger, J. M., and J. W. Sanger. 1980. Banding and polarity of actin filaments in interphase and cleaving cells. *J. Cell Biol.* 86:568–575.

47. Schwartz, S. M., and E. P. Benditt. 1977. Aortic endothelial cell replication. I. Effects of age and hypertension in the rat. *Circ. Res.* 41:248–255.

48. Shibata, N., H. Akagami, K. Tanaka, Y. Okamuro, and M. Oriyama. 1973. A consideration of a mechanism of augmentation of peripheral vascular resistance in hypertension: the presence of F-actin filaments in renal arterioles and electrolyte contents in the arterial wall in hypertensive rats (Goldblatt type). *Jpn. Circ. J.* 37:1285–1291.

49. Smith, T. L., and P. M. Hutchins. 1979. Central hemodynamics in the developmental stage of spontaneous hypertension in the unanesthetized rat. *Hypertension (Dallas).* 1:508–517.

50. Weber, K., and U. Gröschel-Stewart. 1974. Antibody to myosin: the specific visualization of myosin-containing filaments in nonmuscle cells. *Proc. Natl. Acad. Sci. USA.* 71:4561–4564.

51. Wehland, J., M. Osborn, and K. Weber. 1979. Cell to substratum contacts in living cells, a direct correlation between interference reflexion and indirect immunofluorescence microscopy using antibodies against actin and alpha-actinin. *J. Cell Sci.* 37:257–273.

52. Weibel, E. R., and G. E. Palade. 1964. New cytoplasmic components in arterial endothelium. *J. Cell Biol.* 23:101–112.

53. White, G. E., and K. Fujiwara. 1983. Stress fiber expression in vascular endothelial cells in situ: the effects of age, blood pressure, anatomical location, and fluid shear stress. *J. Cell Biol.* 97(5, Pt. 2):267*a*. (Abstr.)

54. White, G. E., K. Fujiwara, E. Shefton, C. F. Dewey, Jr., and M. A. Gimbrone, Jr. 1982. Fluid shear stress influences cell shape and cytoskeletal organization in cultured vascular endothelium. *Fed. Proc.* 41:321 (Abstr.)

55. White, G. E., M. A. Gimbrone, Jr., and K. Fujiwara. 1983. Factors influencing the expression of stress fibers in vascular endothelial cells *in situ*. *J. Cell Biol.* 97:416–424.

56. Wong, A. J., T. D. Pollard, and I. M. Herman. 1983. Actin filament stress fibers in vascular endothelial cells *in vivo*. *Science (Wash. DC).* 219: 867–869.

57. Yamori, Y. 1983. Physiopathology of the various strains of spontaneously hypertensive rats. *In* Hypertension. J. Genest, O. Kuchel, P. Hamet, M. and M. Canter, editors, McGraw-Hill, Inc., New York. 556–581.